ANALYSES OF ENERGY LOSSES AND ACCUMULATOR AND PARAMETERS DESIGN METHOD OF HYDRAULIC IMPACTOR MECHANISM①

He, Qinghua
Department of Mechanical Engineering,
Central South University of Technology, Changsha 410083

ABSTRACT Based on using the formulae derived in reference[1] and thoroughly analyzing of various energy losses of hydraulic impact mechanism, the formulae for calculating mechanical efficiency, volume efficiency and total efficiency were derived. The influence of the acceleration ratio β on the efficiency was analyzed too. In addition the design method of a hydraulic impact mechanism has been introduced.

Key words volume efficiency mechanical efficiency total efficiency accumulator design

1 ENERGY LOSSES AND EFFICIENCY

1.1 *Energy Losses Caused by Local Pressure Losses(E_c)*

Comparing with the local pressure losses caused by complex oil lines inside a hydraulic impact mechanism the pressure drop of the short lines is negligible. Since the pressure drop is proportional to the square of the maximum flow rate, the maximum return speed (u_{rm}) and the maximum impact speed (u_{im}) have the greater influence on the local pressure losses. Therefore, let A be the mean inner section area and ξ the local pressure loss coefficient, the local energy loss (E) of the Double Control (DC) impact mechanism during one impact with a piston moving speed u and at a moving time t_i is

$$E = \int_0^{t_i} 0.5\xi\rho(A_r u|A)^2 Q_{in}\mathrm{d}t = \frac{\xi\rho A_r^2 u_{im}^2 Q_{in} t_i}{6A^2} = \frac{4\xi\rho\psi_{Ar}^2\psi_{sp}E_i^2 Q_{in}}{3A^2R_{in}^2T} \quad (n1)^②$$

where (including the succeeding formulae) the characters without denoted have need to refer paragraph 4 of the paper and Ref. [1].

Accordingly the energy loss in one impact cycle (E_c) and local resistance loss coeficient (φ_c) are, respectively

$$E_c = \varphi_c E_i^2 Q_{in}/p_{in}^2 T \quad (n2)$$

$$\varphi_c = \begin{cases} \{4\xi\rho\psi_{sp}\psi_{Ar}[\beta_2^2\psi_{ur}^3 + \beta(1-\beta_2)^2(1 \\ +\beta_1\psi_{ur}^3)]\}/(3\beta A^2) \quad (RC) \\ \{4\xi\rho\psi_{sp}\psi_{Ar}[\beta_2^2\psi_{ur}^3 + \beta(1 \\ +\beta_1\psi_{ur}^3)]\}/(3\beta A^2) \quad (DC) \end{cases} \quad (n3)$$

1.2 *The Energy Losses Caused By Return Oil Resistance(E_o) And Comprehensive Resistance(E_y)*

E_o can be calculated as following assuming that the return oil resistance is formed in the chamber to which oil returns.

$$E_o = \varphi_o E_i \quad (n4)$$

where φ_o —retum oil loss coefficient

$$\varphi_o = \begin{cases} 2k_o\psi_w^2\psi_{Ar}\psi_{sp}/\beta \quad (RC) \\ 2k_o(1+\beta_2-\beta_1\psi_{ur}^2)\psi_{Ar}\psi_{sp} \quad (DC) \end{cases} \quad (n5)$$

E_y can be calculated as following assuming that resistance is formed in the chamber where the piston cavity is charged with high-pressure oil.

$$E_y = \varphi_y E_i \quad (n6)$$

① Received Sep. 25, 1994; ② Hereafter the formulae number in this paper are sequenially denoted by (n1), (n2), n(3), ···, (n23) to be differed from those of Ref. [1]

$$\varphi_y = \begin{cases} 2k_y(1 + 2\beta_2 \\ + \beta_1\psi_{ur}^2)\psi_{Ar}\psi_{sp} \quad (RC) \\ 2k_y[1 + (\beta_1 \\ + \beta_2/\beta)\psi_{ur}^2\psi_{sp} \quad (DC) \end{cases} \tag{n7}$$

1.3 *Energy Losses Caused by Leakage* (E_l)

$$E_l = V_l p_{in} = \varphi_l p_{in}^2 T \tag{n8}$$

where φ_l —oil leakage coefficient

$$\varphi_l = \begin{cases} k_{fl} + 2k_{rl}\psi_{sp}(1 \\ + \beta_1\psi_{ur}) \quad (RC) \\ 2\psi_{sp}[k_{fl}\psi_{ur}/\beta + k_{rl}(1 \\ + \beta_1\psi_{ur})] \quad (DC) \end{cases} \tag{n9}$$

1.4 *Energy Losses Caused By Unretrieved Oil* (E_u)

$$E_u = V_u p_{in} = \varphi_u E_i \tag{n10}$$

where φ_u —energy loss coefficient due to diminution of travel longth of piston

$$\varphi_u = \begin{cases} 2\psi_{Ar}\psi_{sp}(\beta_2 - {}_1\psi_{ur}^2) \quad (RC) \\ 2\psi_{Ar}\psi_{sp}\psi_{ur}^2(\beta_2/\beta - \beta_1) \quad (DC) \end{cases} \tag{n11}$$

1.5 *Volume Efficiency* (η_v), *Mechanism Efficiency* (η_m), *Pressure Efficiency* (η_p) *and Total Efficiency*(η)

$$\eta_v = \frac{V_e}{V_e + V_u + V_l} = \begin{cases} \dfrac{(A_r - A_f)s_p}{A_f s_r + \varphi_l p_{in} T} \quad (RC) \\ \dfrac{A_r s_p}{(A_r + A_f)s_r + \varphi_l p_{in}} \quad (DC) \end{cases} = \begin{cases} \dfrac{2\beta(1 - \beta_2)\psi_{Ar}\psi_{sp}E_i}{2\psi_{Ar}\psi_{sp}\psi_{ur}^2 E_i + \psi_l\beta p_{in}^2 T} \quad (RC) \\ \dfrac{2\beta\psi_{Ar}\psi_{sp}E_i}{2(1 + \beta_2)\psi_{Ar}\psi_{sp}\psi_{ur}^2 E_i + \varphi_l\beta p_{in}^2 T} \quad (DC) \end{cases} \tag{n12}$$

For the sake of convenience, the input oil pressure (p_{in}) used precedently doesn't actually include the average pressure drop caused by local resistance.

$$\Delta p_c = E_c/(Q_{in}T) \tag{n13}$$

The total input hydraulic energy E_{in} and efficiency η_m during one cycle are

$$E_{in} = E_i + E_c + E_l + E_y + E_o \tag{n14}$$

$$\eta_m = 1 - (E_o + E_y)/E_{in} \tag{n15}$$

On the basis of data calculated from formula(n18), Fig. 1 and Fig. 2 are drawn to illustrate the relationship among β_1, p_{in} and η of DC and RC. In these figures the grids illustrate the variance of η.

Fig. 1(a), 1(b) are based on the relationship among η, p_{in}, and β at relatively greater energy losses. However, in Fig. 1(c), 1(d) the energy losses are smaller. In these figures a maximum value of total efficiency is existed respectively.

To reveal the distribution of efficiency contour lines the projections of Figs. 1(a)~1(d) on X-Y plane are drawn in Fig. 2. From Fig. 2 it can be seen that with the variance of energy losses the efficiencies change and the distributions of high-efficiency zones also, move toward the areas with greater β and p_{in}.

η_p and η can be calculated as following:

$$\eta_q = 1 - E_o/E_{in} \tag{n16}$$

$$\eta = E_i/E_{in} = E_i/(E_i + E_o + E_l + E_y + E_o) \tag{n17}$$

Using formula(31) of Ref. [1] and φ_y, φ_o, φ_l, the η can also be calculated as:

$$\eta = (E_i T^2 p_{in}^3)/[\varphi_l T^3 p_{in}^3 + (1 + \varphi_y + \varphi_o)E_i T^2 p_{in}^3 + \varphi_l\varphi_c E_i^2 T p_{in} + \varphi_l\varphi_q E_i^3] \tag{n18}$$

Based on the preceding analysis, η can be concluded as a function of β and p_{in} of a hydraulic impact mechanism at a given impact energy E_i, impact frequency $1/T$ and p_{in} (where T is the time of one impact cycle).

2 EFFICIENCY ANALYSIS

Based on the analysis of the energy losses and formula (n18), the influence exerted by β and p_{in} on the energy efficiency is discussed graphically(refer to Fig. 2). All the figures are based on an example mechanism with the impact energy 500 J and impact frequency 30 Hz. In the following analysis all the parameters except that being discussed remain unchanged.

Compared with the little influence on the efficiency contour lines exerted by K_y, K_o the influence by ξ is greatest, resulting in a ridge like curved line of efficiency contour instead of maximum values on the topography of the ef-

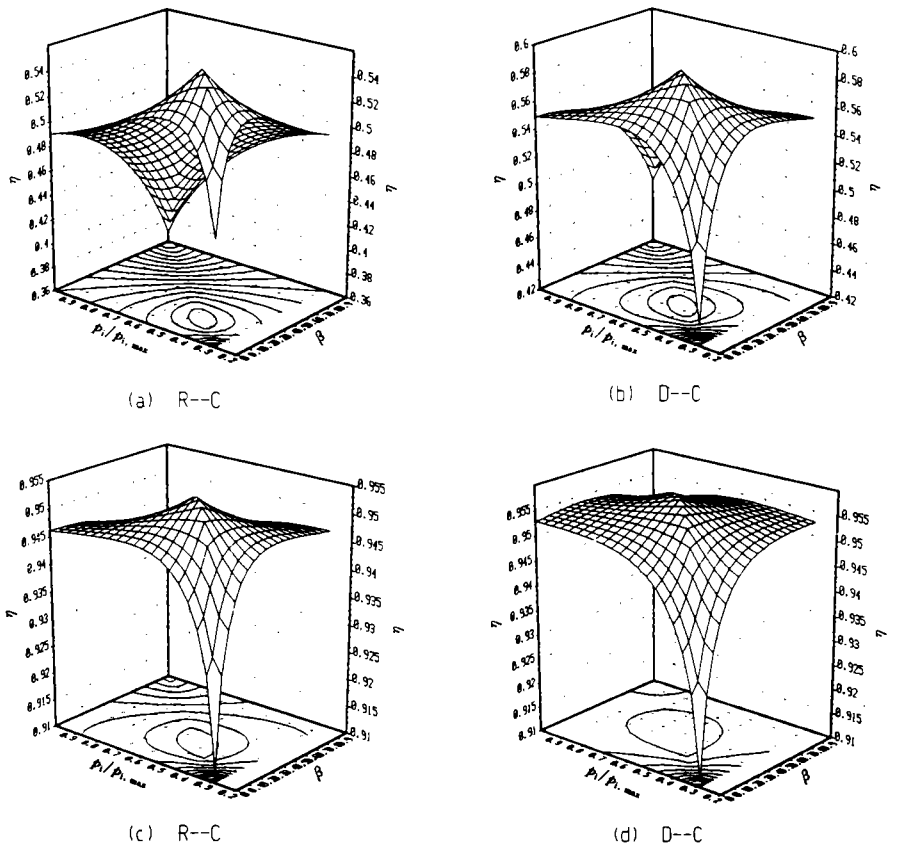

Fig. 1 Relationship between η, P_{in} and β

ficiency contour surface. Parameter K_1 causes the high-efficiency zone being shifted to the area with greater β and p_{in}.

Totally, the relationship among η, β and P_{in} can be summarized as following:

(1) There is a high-efficiency zone. And η decreases when β, p_{in} are too small or too high.

(2) The high-efficiency zone of RC is in the area where $\beta = 0.15 \sim 0.50$, $p_{in}/p_{in\,max} = 0.38 \sim 0.64$. And the high-efficiency zone of DC is in the area where $\beta = 0.24 \sim 0.70$, $p_{in}/p_{in\,max} = 0.45 \sim 0.82$.

(3) Under equal conditions, the efficiency of RC is lower than that of DC. However the distribution density of DC curves is smaller.

(4) Efficiency doesn't decrease significantly even in the area to be quite off the high-efficiency zone.

(5) Since the high-efficiency zone is quite wide and insensitive to β and p_{in}, it is not necessary and practical to seek for a set of optimum design with the maximum efficient.

3 OIL CHARGING AND DISCHARGING IN ACCUMULATOR AND ACCELERATION RATIO β

The accumulator is vital to the performance of hydraulic impact mechanism. It is a special kind of membrane accumulator with the membrane vibrating thousands of times in a second.

To reduce the oil charging/discharging frequency and charged/discharged oil volume, relationship between accumulator and mechanism parameters will be discussed and investigated thoroughly and practically (Fig. 3).

3.1 *The Oil Charging and Discharging Frequency*

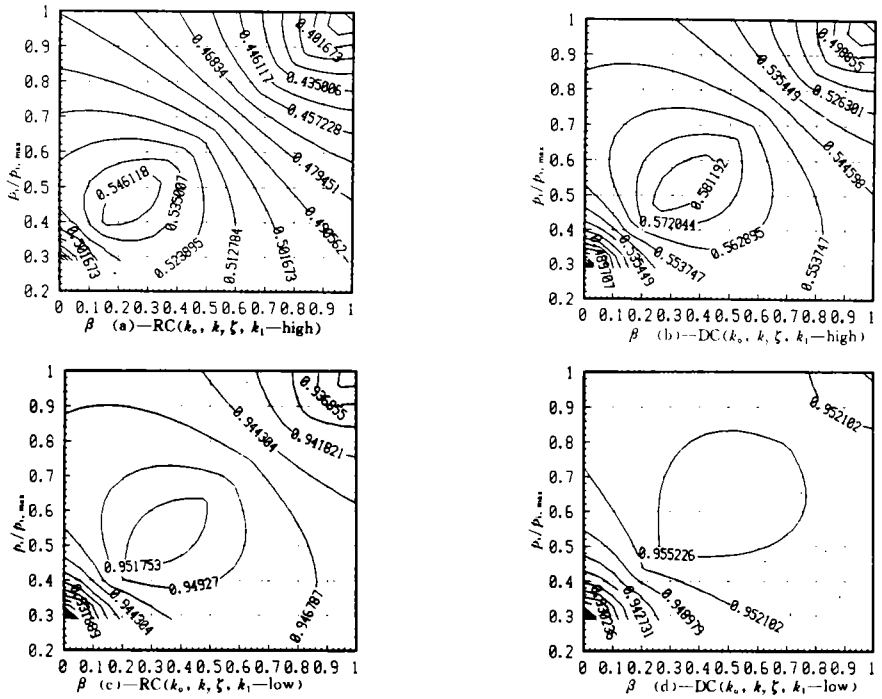

Fig. 2 Distribution of efficiency contour lines

Under normal conditions, the accumulator is charged and discharged with oil twice respectively during one cycle. However, according to the analysis in Ref. [1], the membrane vibrates just once during one cycle if the design fits formula (37).

It therefore can prolong the service life of the membrane.

Under ideal working conditions, formula (37) in Ref. [1] can be formulated as

$$\beta/(1+\beta) - \psi_{ur}\psi_{sp}/\beta \leqslant 0 \qquad \text{(n19)}$$

$$\beta^* \leqslant 1/3 \qquad \text{(n20)}$$

where β^* —feature value of oil charging/discharging freguency, refer to section of 3.2.

Under practical condition, β decreases as K_o and K_y increase.

3.2 *The Minimum Charged/Discharged Oil Volume and Feature Values β^*, β^{**}*

The relationship among charged and discharged oil volume ΔV_i and ΔV_o of RC and DC accumulator and return acceleration ratio β has been illustrated in Fig. 3(a). In the overlapped part ($\beta < 1/3$) of the two curves, the accumulator is charged and discharged with oil only once respectively. The abscissa value of the end point of overlapped part is designated as β^*. During this part ΔV_i and ΔV_o decrease as β increases. While β^* and ΔV_o continue to decrease gradually, ΔV_i increases abruptly after a sudden decrease and then crosses the oil-discharging curve. Since the designed discharging oil volume (ΔV_a) is the smaller of the two, the cross point is the minimum of the designed discharging oil volume. Therefore the return acceleration β at the intersection is the other feature value, specified as β^{**}. Relationship between ΔV_a and β is illustrated in Fig. 3(b).

Based on the result of calculation, it can be seen that β^{**} is affected by comprehensive resistance coefficient (K_y), return resistance coefficient (K_o). Normally β^{**} increases as K_y increases. In Fig. 4 the relationship among them is illustrated topographically.

β^{**} can be worked out on computer numerically based on formula(n21) and the con-

ception descibed directly above.

$$\begin{cases} 2(1+\beta_1\psi_{ur})\psi_{ur}^2\psi_{sp} - \beta(1 \\ -\beta_1)(1-\beta_r\psi_{ur}^2) = 0 \quad (RC) \\ 2(1+\beta_o)(1+\beta_1\psi_{ur})\psi_{ur}^2\psi_{sp} - \beta(1 \\ -\beta_1\psi_{ur}^2) = 0 \quad (DC) \end{cases} \tag{n21}$$

Under ideal working conditions formula (n21) is expressed as

$$(\psi_{sp}+\psi_{ur})^2 = (1-\psi_{sp})^2 \tag{n22}$$

and formula(n22) can be further simplified as

$$\beta^2+\beta-1=0$$

and then get

$$\beta^{**} = (\sqrt{5}-1)/2 \approx 0.618 \tag{n23}$$

In addition, the relationsahips befween k_y, k_o and β^*, β^{**} are figured in Table 1.

3.3 *Selection of Acceleration Ratio*(β)

Following discussion is concentrated on selecting β according to actual conditions.

On the basis of the data in Table 1, it can be concluded that to reduce the vibrating frequency of membrane taking $\beta < 1/3$ and $\beta^{**} > 0.618$ are suitable, however it is impossible to meet those two requirements at the same time. To solve the above contradiction, it is necessary to look back Fig. 3(b) of which, ΔV_a decreases evenly at frist with the increasing of β value, while changes much abruptly when it is off the zone of $\beta < 1/3$ especially when $\beta > \beta^{**}$. Thus the characteristics of an accumulator working between these two feature values can be summarized as follows.

Table 1 Relationship between K_y, K_o and β^* and β^{**}

K_o	K_y	β^*		β^{**}	
		RC	DC	RC	DC
0	0	0.333	0.333	0.618	0.618
0.02	0.02	0.322	0.326	0.624	0.618
0.04	0.04	0.310	0.319	0.631	0.618
0.06	0.06	0.297	0.312	0.638	0.619
0.08	0.08	0.283	0.303	0.646	0.619
0.10	0.10	0.268	0.294	0.655	0.620
0.12	0.12	0.251	0.283	0.665	0.620

(1) Little oil is discharged during the return acceleration stage.

(2) ΔV_a increases gradually as β increases. The membrane accumulator adopted in hydraulic impact mechanism is generally platformed. Therefore the volume of charged/discharged oil is the multiple of the area of membrane and offset between oil charging and discharging(Δh), i.e. $\Delta V = A_a \Delta h$.

When the increase of ΔV is small the membrane of the accumulator doesn't move essentially. Therefore when β is between β^* and β^{**}, it doesn't actually influence the oil charging/discharging frequency and ΔV_a. On the basis of analyzing the high-efficiency zone, it is advisable to select β between 0.36 and 0.55. If β is too small, the areas of the front and rear chambers differ greatly, causing disadvantages to energy transferring and piston. If β is too high, efficiency decreases.

4 THE APPLICATION OF THREE-STAGE ANALYSIS METHOD IN DESIGNING HYDRAULIC IMPACT MECHANISM

The procedures of designing a hydreulic impact mechanism using the three-stage method[1] are listed as following:

(1) Determine impact energy(E_i), impact frequency(f) and input oil pressure(p_{in} including local resistance pressure drop).

(2) Select the maximum impact speed (u_{im}) (Generally between 6m/s and 10m/s).

(3) Select return oil resistance coefficient K_o (0.05～0.12) and comprehensive return oil resistance coefficient K_y (0.06～0.12).

(4) Compute the leakage coefficient k_{rl} and k_{fl} of front and rear chamber respectively using leakage formulae for eccentricly circular gap(eccentricity rate 0.8—0.95).

(5) Determine ξ between 180 and 140 and diameter of oil lines(the value of ξ is based on experiences due to the complicated oil lines inside the mechanism).

(6) Calculate feature values β^* and β^{**} using formulae (37) and (n21)

(7) Determine β_1 and β_2 using formulae (24) and (21)

(8) Determine other parameters using the

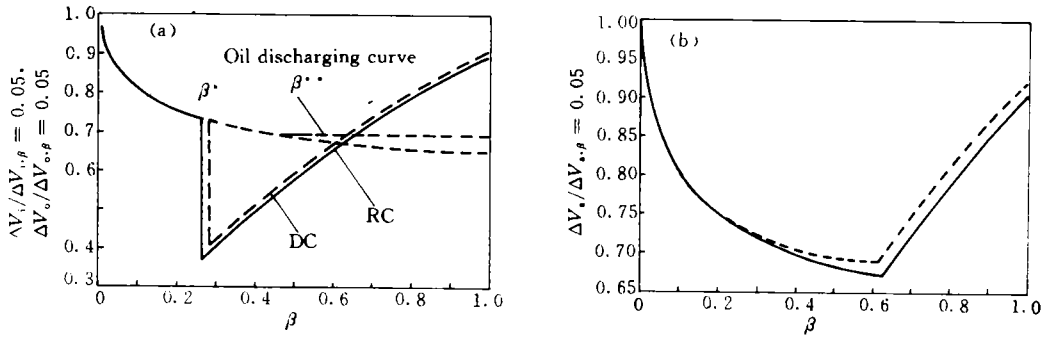

Fig. 3 Relationship between β and charged/discharged oil volume

dash line—DC; solid line—RC

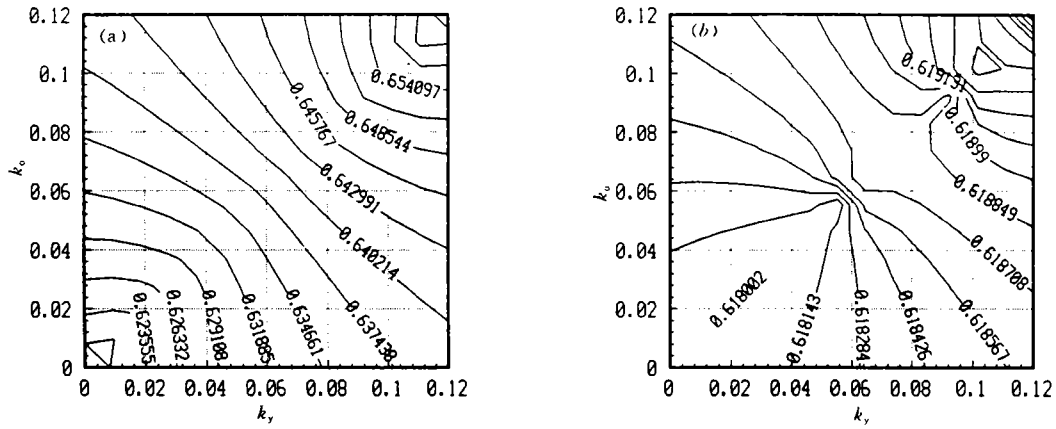

Fig. 4 Influence of k_y and k_o on feature values β''

corresponding formulae:

determing mass of piston(m_p) using formula (3)

determing ψ_{sp} and S_p using (1), (5)

determing ψ_{ur} and maximum return speed (u_{rm}) using (2), (11)

determing return control oil port (S_{rc}) and impact control oil port (S_c) by (15), (16)

determing area coefficients (ψ_{Ar}) and (ψ_{Af}) for rear and front chamber respectively by (19), (20)

determing total local energy loss (E_c) and coefficient ψ_c by (n2), (n3)

determing return oil energy loss(E_o) and coefficient ψ_o by (n4), (n5)

determing comprehensive resistance energy loss(E_y) and coefficient ψ_y by (n6), (n7)

determing total leakage energy loss(E_l) and coefficient ψ_l by (n8), (n9)

determing input oil flow(Q_{in}) by (31)

determing oil pressure drop caused by local pressure loss(ΔP_c) by (n13)

determing finally Q_{in} using $P_{in} - \Delta P_c$ (not including the oil used by control valves, generally 10% of Q_{in}). determine total input oil flow 1.08—1.12 Q_{in}

determing ΔV_a by (34), (35), here ΔV_a is the bigger results of these two formulae.

determing areas of front and rear chamber A_r and A_f respectively using(22), (23)

determing total efficiency(η) (if the energy consumed by control valves are taken into consideration η should be divided by a coefficient between 1.08~1.11) using(n18)

5 CONCLUSION

(1) The derivations of the formulae for energy losses and analysis of relationship among β, P_{in} and total efficiency are of practical value in optimizing hydraulic impact mechanisms.

(2) On analyzing the two feature values of accumulators the motion laws of the mechanism are revealed thoroughly.

(3) The computing procedures introduced in the paragraph above is of convenience in determining the parameters of the mechanism precisely.

REFERENCE

1 He Qinghua, Transactions of Nonferrous Metals Society of China, 1995, 5(1), 116—121.

(*From page 127*) compared to the preheated powders. With the progressing of the extrusion, temperature rise is more considerable and the powders in the extrusion container are heated for more time, so more dispersoids precipitate.

However, considering the fact that the coarsening rate of $Al_{12}(Fe, V)_3Si$ dispersoids is very small and the the duration of the extrusion processing is also relatively short, it is not enough to explain the clear coarsening of the dispersoids only by the temperature rise. The precipitate coarsening rate is given by[7]:

$$dr/dt = Dc\sigma r^{-2} \quad (2)$$

where r is the precipitate size; D is the solid diffusion coefficient; c is the equillibrium solubility; σ is the interfacial energy between the matrix and the precipitate.

The measurement of the coarsening rate as described is usually carried out in the case without applied stress on the precipitates. It is apparent, however, that very high extrusion force exists during extrusion, which is necessarily considered in the calculation of the coarsening rate. The coarsening rate is directly proportional to the solid diffusion coefficient D. It is well accepted that atoms can diffuse by transgressing the potential barrier with the help of heat activation if there exists chemical potential gradient of the solute constituent in the solid solution. However, diffusion can also occur if stress exists, even if the solute atoms are uniformly distributed. The increment of the solute flux because of the applied stress can be thought to correspond with the improvement of diffusion coefficient D in equation (1), leading to faster coarsening rate compared to that without stress. Therefore, the clear coarsening of the precipitates in the late stage of extrusion is possible on account of the effect of temperature rise and high stress regardless of the low initial coarsening rate.

5 CONCLUSION

(1) The inhomogeneity of the microstructure and properties exists evidently in the extruded, rapidly solidified AlFeVSi material with decreaing mechanical properties, improved size and quantity of the precipitates along the extrusion directon.

(2) The variation of the microstructure might result from the extrusion force in addition to the temperature rise during extrusion.

REFERENCE

1 Franck R E, Hawk J A. Script Metall, 1989, 23: 113.
2 Chen Zhenhua *et al.* CN88212137.5, 1988.
3 Mitra S, Mcnelley T R. Metall Trans, 1993, 24A: 2589.
4 Premkuar M K *et al.* In: Hildeman G J(ed), High Strength Powder Metallurgy Aluminium Alloys Ⅱ, A Publication of the Metallurgical Society, Inc, 1985: 265.
5 Michot G, Champier G. Invited Paper Presented at ICAA2, 1990, Beijing, China.
6 Skinner D J *et al.* Script Metall, 1986, (20): 867.
7 Fighser J C *et al.* Acta Metall, 1953(1).